Role of the intrinsic surface state in the decay of image states at a metal surface

J. Osma
Departamento de Física de Materiales, Facultad de Ciencias Químicas, Universidad del País, Vasco/Euskal Herriko Unibertsitatea, Apartado 1072, 20080, San Sebastián, Basque Country, Spain

I. Sarría
Materia Kondentsatuaren Fisika Saila, Zientzi Fakultatea, Euskal Herriko Unibertsitatea, 644 Posta kutxatila, 48080 Bilbo, Basque Country, Spain

E. V. Chulkov
Departamento de Física de Materiales, Facultad de Ciencias Químicas, Universidad del País, Vasco/Euskal Herriko Unibertsitatea, Apartado 1072, 20080, San Sebastián, Basque Country, Spain
and Centro Mixto CSIC-UPV/EHU, San Sebastián, Basque Country, Spain

J. M. Pitarke
Materia Kondentsatuaren Fisika Saila, Zientzi Fakultatea, Euskal Herriko Unibertsitatea, 644 Posta kutxatila, 48080 Bilbo, Basque Country, Spain
and Centro Mixto CSIC-UPV/EHU, San Sebastián, Basque Country, Spain

P. M. Echenique
Departamento de Física de Materiales, Facultad de Ciencias Químicas, Universidad del País Vasco/Euskal Herriko Unibertsitatea, Apartado 1072, 20080, San Sebastián, Basque Country, Spain
and Centro Mixto CSIC-UPV/EHU, San Sebastián, Basque Country, Spain

(Received 28 May 1998; revised manuscript received 3 November 1998)

The role of the intrinsic surface state ($n=0$) in the decay of the first image state ($n=1$) at the (111) surface of copper is investigated. Inelastic linewidths are evaluated from the knowledge of the imaginary part of the electron self energy, which we compute, within the *GW* approximation of the many-body theory, by going beyond a free-electron description of the metal surface. Single-particle wave functions are obtained by solving the Schrödinger equation with a realistic one-dimensional model potential, and departure of the motion along the surface from free-electron behavior is considered through the introduction of the effective mass. The decay of the first image state of Cu(111) into the intrinsic surface state is found to result in a linewidth that represents 40% of the total linewidth. The dependence of linewidths on the momentum of the image state parallel to the surface is also investigated. [S0163-1829(99)09415-1]

I. INTRODUCTION

The presence of an electron in front of a solid surface redistributes the charge in the solid. As a consequence, an attractive potential is induced, which far from the surface approaches the long-range classical image potential $V_{\rm im}(z) = -g_s/4z$ [z being the distance from the surface, $g_s=(\epsilon_s-1)/(\epsilon_s+1)$, and ϵ_s the static bulk-dielectric constant; for a metal, $g_s=1$]. If the bulk-band structure projected onto the surface presents an energy gap near the vacuum level, an electron located in front of the surface cannot propagate into the solid. Therefore, the electron may be trapped in the vacuum well, and an infinite series of Rydberg-like states appears, which converges, for zero parallel momentum, towards the vacuum energy. These so-called image states[1–3] are localized in the vacuum region of the surface, the penetration of the first ($n=1$) image wave function into the solid varying typically between 4% and 22%.[4] As a result, image states are almost decoupled from bulk-electron scattering, and they are much longer lived than bulk excitations: the lifetime of bulk electrons with energies of 4 eV above the Fermi level is approximately one order of magnitude smaller than that of the first image state. Furthermore, the lifetime of higher-order image states ($n\geqslant 1$) has been predicted[1] to scale asymptotically with n^3, which makes the series to be resolvable.

During the last decade the linewidth of image states has been measured by inverse photoemission,[5,6] two-photon photoemission,[7–9] and time-resolved two-photon photoemission.[10–14] Recently, time-resolved two-photon photoemission has been used in combination with the coherent excitation of several quantum states, and the lifetime of the first six image states on the (100) surface of copper has been accurately determined.[15]

Theoretical calculations of the linewidth of image states were first reported in Refs. 16 and 17, within a many-body free-electron description of the metal surface and with the use of simplified models to approximate both initial and final electronic states and, also, the screened-Coulomb interaction. Later on, the decay of the first image state on the (111) surfaces of copper and nickel metals to the $n=0$ crystal-induced surface state was calculated,[18] in terms of Auger transitions, with the use of a three-band model to describe the surface band structure. In Ref. 18, hydrogeniclike states

with no penetration into the solid were used to describe the image-state wave functions, a simplified parametrized form was used for the surface-state wave functions, and screening effects were neglected. Self-consistent calculations of the linewidths of image states on copper surfaces have been reported recently,[19] and good agreement with experimentally determined decay times has been found. In Ref. 19, the linewidths of image states were computed, within the (*GW*) approximation of the many-body theory,[20] by going beyond a free-electron description of the metal surface. Single-particle wave functions were obtained by solving the Schrödinger equation with a realistic one-dimensional model potential,[21] and the screened interaction was evaluated in the random-phase approximation (RPA).[22]

In this paper we focus our attention on the role that the crystal-induced surface state ($n=0$) plays in the relaxation of the first image state at the (111) surface of copper, which we find to represent 40% of the total linewidth. We present self-consistent calculations along the lines of Ref. 19, and we also consider simplified models for both the electronic wave functions and the screened-Coulomb interaction, showing that a detailed description of these quantities is of crucial importance in the understanding of the origin and magnitude of linewidths of image states. We account for potential variation parallel to the surface through the introduction of the effective mass, and we find that the linewidth of the first image state of Cu(111) is 20% smaller than in the case of free-electron behavior along the surface. Finally, we investigate the dependence of interband[23] linewidths on the momentum of the image state parallel to the surface $\mathbf{k}_\parallel$. Our results indicate that for image state total energies lying below the top of the gap, the linewidth of the first image state of Cu(111) is increased with $\mathbf{k}_\parallel \neq 0$ up to 20%.

II. THEORY

We assume translational invariance in the plane parallel to the surface, which is taken to be normal to the z axis, and we evaluate the inelastic linewidth of the image state $\phi_1(z)e^{i\mathbf{k}_\parallel\cdot\mathbf{r}_\parallel}$ with energy $E_1=\epsilon_1+\mathbf{k}_\parallel^2/(2m_1)$ (Ref. 24) (we use atomic units throughout, i.e., $e^2=\hbar=m_e=1$), as the projection of the imaginary part of the electron self-energy $\Sigma(\mathbf{r},\mathbf{r}';E_1)$, over the state itself:

$$\Gamma=-2\int dz\,dz'\,\phi_1^*(z)\,\mathrm{Im}\,\Sigma(z,z',\mathbf{k}_\parallel;E_1)\,\phi_1(z'), \quad (1)$$

where $\Sigma(z,z',\mathbf{k}_\parallel;E_1)$ represents the two-dimensional Fourier transform of $\Sigma(\mathbf{r},\mathbf{r}';E_1)$.

In the *GW* approximation,[20] the self-energy is obtained by just keeping the first term of the expansion in the screened interaction (W). Then, after replacing the Green function by the zero-order approximation, one finds

$$\mathrm{Im}\,\Sigma(z,z',\mathbf{k}_\parallel;E_1)=\sum_{E_F\le E_f\le E_1}\int\frac{d^2\mathbf{q}_\parallel}{(2\pi)^2}\,\phi_f^*(z') \times \mathrm{Im}\,W^{\mathrm{ind}}(z,z',\mathbf{q}_\parallel;E_1-E_f)\,\phi_f(z), \quad (2)$$

where the sum is extended over a complete set of final states $\phi_f(z)e^{i(\mathbf{k}_\parallel+\mathbf{q}_\parallel)\cdot\mathbf{r}_\parallel}$ with energies $E_f=\epsilon_f+(\mathbf{k}_\parallel+\mathbf{q}_\parallel)^2/(2m_f)$. m_f is the effective mass, which accounts for the departure of the motion along the surface from free-electron behavior, E_F is the Fermi energy, and $W^{\mathrm{ind}}(z,z',\mathbf{q}_\parallel,E)$ represents the two-dimensional Fourier transform of the induced part of the screened interaction.

In particular, if only transitions into the crystal-induced $n=0$ surface state $\phi_0(z)e^{i(\mathbf{k}_\parallel+\mathbf{q}_\parallel)\cdot\mathbf{r}_\parallel}$ with energy $E_0=\epsilon_0+(\mathbf{k}_\parallel+\mathbf{q}_\parallel)^2/(2m_0)$ are considered, one finds

$$\mathrm{Im}\,\Sigma_s(z,z',\mathbf{k}_\parallel;E_1)=\int\frac{d^2\mathbf{q}_\parallel}{(2\pi)^2}\,\phi_0^*(z') \times \mathrm{Im}\,W^{\mathrm{ind}}(z,z',\mathbf{q}_\parallel;E_1-E_0)\,\phi_0(z), \quad (3)$$

and introducing this contribution to $\mathrm{Im}\,\Sigma(z,z',\mathbf{k}_\parallel;E_1)$ into Eq. (1) one finds

$$\Gamma_s=-2\int\frac{d^2\mathbf{q}_\parallel}{(2\pi)^2}\int dz\,dz'\,\phi_1^*(z)\,\phi_0^*(z') \times \mathrm{Im}\,W^{\mathrm{ind}}(z,z',\mathbf{q}_\parallel;E_1-E_0)\,\phi_0(z)\,\phi_1(z'). \quad (4)$$

Three different models have been used for the evaluation of the screened interaction W. First, the specular-reflection model (SRM) of Ritchie and Marusak[25] has been considered. In this model, bulk electrons are assumed to be specularly reflected at the surface, the interference between the ingoing and outgoing waves being neglected, and the electronic charge density abruptly terminates at the surface ($z=0$), which we choose to be located half a lattice spacing beyond the last atomic layer. Within this simplified model,[26] also called semiclassical infinite barrier model the screened interaction is obtained in terms of the wave-vector and frequency-dependent bulk-dielectric function, which we evaluate in the RPA. Second, for the vacuum contribution to the linewidth ($z>0$, $z'>0$) the surface response function suggested by Persson and Zaremba[27] (PZ) has been used. Finally, the screened interaction has been evaluated, as in Ref. 19, by solving the RPA integral equation for the density-response function of inhomogeneous media in terms of the eigenfunctions of the one-electron effective Hamiltonian. These eigenfunctions have been computed by solving the Schrödinger equation with the realistic one-dimensional model potential suggested in Ref. 21. This model potential uses as parameters the width and position of the energy gap at the Γ point ($\mathbf{k}_\parallel=0$) and, also, the binding energies of both the $n=0$ crystal-induced surface state at Γ and the first image state.

For the evaluation of $n=0$ and $n=1$ surface states, we have first used simplified models for the wave functions inside and outside the solid. In the vacuum side of the surface ($z>0$), $n=1$ and $n=0$ states have been approximated by a parametrized $1s$-like hydrogenic wave function and a mere exponential, respectively, which have been matched to a decaying wave function in the crystal band gap ($z<0$) obtained within a nearly-free-electron two-band model:[17]

$$\phi_n(z<0)\sim e^{\Delta_n z}\cos(Gz+\delta_n). \quad (5)$$

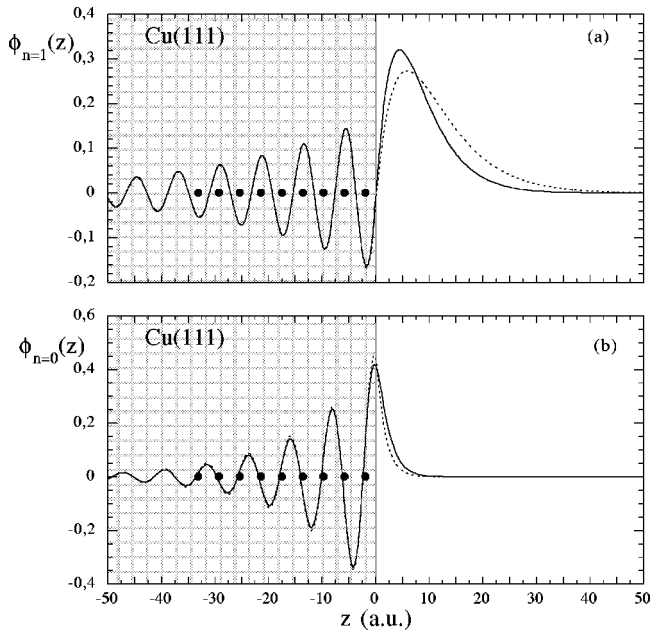

FIG. 1. Wave functions of both (a) $n=1$ image and (b) $n=0$ intrinsic surface states on Cu(111), as obtained within two different models: MWF (solid line) and AWF (dotted line) (see text). Full circles represent the atomic positions in the (111) direction. The geometrical electronic edge ($z=0$) has been chosen to be located half an interlayer spacing beyond the last atomic layer. Notice the *s*-like and *p*-like characters of the image and intrinsic-surface-state wave functions, respectively.

Here, $n=0$ and $n=1$ correspond to the crystal-induced surface state and the first image state, respectively, G is the limit of the Brillouin zone in the direction normal to the surface, and

$$\Delta_n=\frac{1}{G}\sqrt{\frac{1}{4}E_{\mathrm{gap}}^2-\overline{\epsilon}_n^2}, \tag{6}$$

where E_{gap} and $\overline{\epsilon}_n$ represent the energy gap and the energy of the n surface state with respect to the midgap, respectively. The phase shift δ_n is given by

$$\delta_n=\frac{1}{2}\times\begin{cases}\pi-\tan^{-1}\left[\sqrt{\dfrac{1}{\eta_n^2}-1}\right], & \text{if } 0\leqslant\eta_n\leqslant 1\\ \tan^{-1}\left[\sqrt{\dfrac{1}{\eta_n^2}-1}\right], & \text{if } -1\leqslant\eta_n\leqslant 0,\end{cases} \tag{7}$$

with $\eta_n=2\overline{\epsilon}_n/E_{\mathrm{gap}}$.

The image state on Cu(111) is located right at the top of the gap ($\delta_1\simeq 0.9\times\pi/2$), both the hydrogeniclike wave function in the vacuum ($z>0$) and the decaying *s*-like wave function in the bulk ($z<0$) having, therefore, nodes at the surface ($z=0$). The $n=0$ crystal-induced surface state on Cu(111) is located at the bottom of the gap ($\delta_0\simeq 0.2\times\pi/2$); thus, it is described by a *p*-like wave function in the bulk. These approximate wave functions (AWF) are exhibited in Fig. 1, together with the corresponding wave functions that we obtain by solving the Schrödinger equation with the one-dimensional potential of Ref. 21 [model wave functions (MWF)]. Both wave functions, AWF and MWF, coincide within the bulk, but the hydrogeniclike wave function for the $n=1$ image state appears to be less localized near the surface than our model wave function. The $n=0$ and $n=1$ surface states on Cu(111) have binding energies (measured with respect to the vacuum level) of 0.83 and 5.32 eV, respectively. The $n=1$ probability density has a maximum at 4.3 a.u. outside the crystal edge ($z=0$). The penetration into the bulk of $n=0$ and $n=1$ surface states is found to be, at the $\overline{\Gamma}$ point, of 74.5% and 22.1%, respectively.

TABLE I. Calculated linewidth (in meV) coming from the decay of the $n=1$ image state on Cu(111) into the $n=0$ intrinsic surface state, as obtained within three different models for the description of the surface response and two different models for the description of both initial and final wave functions (see text). RPA accounts for our full RPA realistic calculation of the screened interaction, SRM for the simplified specular reflection model of Ritchie and Marusak (Ref. 25), and PZ for the vacuum side surface response suggested by Persson and Zaremba (Ref. 27). MWF accounts for the wave functions obtained by solving the Schrödinger equation with the realistic one-dimensional model potential of Ref. 21, and AWF for the approximate model described in the text. The effective mass of the $n=1$ image state has been set equal to the free-electron mass, and for the $n=0$ surface state we have used either $m_0=1$ or $m_0=0.42$. The momentum of the image electron parallel to the surface is set equal to zero.

Surf. Res.	Wave function	Γ_{vac}	Γ_{sol}	Γ_{inter}	Γ_s
RPA($m_0=1$)	MWF	42	16	−42	16
RPA($m_0\neq 1$)	MWF	29	8	−25	12
SRM($m_0=1$)	MWF	11	12	−17	6
SRM($m_0=1$)	AWF	2	15	−9	8
PZ($m_0=1$)	MWF	55			
PZ($m_0=1$)	AWF	12			

III. RESULTS AND DISCUSSION

The results of our calculations for the linewidth Γ_s, coming from the decay of the $n=1$ image state into the $n=0$ intrinsic surface state on Cu(111) are presented in Table I, with the momentum of the image electron parallel to the surface $\mathbf{k}_\parallel$ set equal to zero. Here, the linewidth has been split as follows:

$$\Gamma_s=\Gamma_{\mathrm{vac}}+\Gamma_{\mathrm{sol}}+\Gamma_{\mathrm{inter}}, \tag{8}$$

where Γ_{vac}, Γ_{sol}, and Γ_{inter} represent vacuum, bulk, and interference contributions, respectively, as obtained by confining the integrals in Eq. (4) to either vacuum ($z>0,z'>0$), bulk ($z<0,z'<0$), or vacuum-bulk ($z\gtrless 0,z'\lessgtr 0$) coordinates. First we show our full RPA calculations, in which the screened interaction is obtained on the basis of one-electron eigenfunctions computed from the realistic one-dimensional model potential of Ref. 21. Within these calculations both $n=0$ and $n=1$ surface-state wave functions are also obtained from the model potential of Ref. 21 (MWF), with either $m_0=1$ or $m_0=0.42$.[28–30] Within the specular reflection model[31] and the model suggested by Persson and

TABLE II. Calculated total linewidth (in meV) coming from the decay of the $n=1$ image state on Cu(111) into any unoccupied final state with $E_f<E_1$, as obtained within our full RPA scheme with all wave functions computed from the one-dimensional model potential of Ref. 21. As in Table I, the effective mass and the momentum parallel to the surface of the $n=1$ image state have been set equal to the free-electron mass and equal to zero,respectively. As for final (bulk and intrinsic surface) states, we have used either $m_f=1$ or the realistic effective masses ($m_f=1$) described in the text. Contributions to the linewidth from decay into bulk states $\Gamma-\Gamma_s$ are displayed in parentheses.

Surf. Res.	Γ_{vac}	Γ_{sol}	Γ_{inter}	Γ
RPA($m_f=1$)	47(5)	44(28)	$-54(-12)$	37(21)
RPA($m_f\neq1$)	34(5)	32(24)	$-37(-12)$	29(17)

Zaremba[32] for the screened interaction, we have used the MWF $n=0$ and $n=1$ surface-state wave functions as well as the simplified models (AWF) described in the previous section, with $m_0=1$.

Total linewidths Γ, as obtained from the decay of the $n=1$ image state on Cu(111) into any final state with energy $E_f,E_F\leqslant E_f\leqslant E_1$, [see Eqs. (1) and (2)], are presented in Table II. Here, our full RPA calculations are shown, with all wave functions computed from the one-dimensional model potential of Ref. 21 (MWF). Realistic values of the effective mass of final states have been considered, according to the experiment or to *ab initio* band-structure calculations. As for the $n=0$ surface state, we have used $m_0=0.42$, as in Table I, and for bulk states we have chosen to increase the effective mass from our computed value[33,34] of $m_f=0.22$ at the bottom of the gap to $m_f=1$ at the bottom of the valence band.

Our full RPA calculations indicate that the decaying rate of the $n=1$ image state into the $n=0$ crystal-induced surface state results for $m_0=1$ in a linewidth of 16 meV, while use of the more realistic effective mass $m_0=0.42$ leads to a linewidth of 12 meV. With the use of either the free-electron mass or more realistic effective masses for both bulk and crystal-induced surface states, Γ_s approximately represents 40% of the total linewidth, $\Gamma=37$ meV ($m_f=1$) or $\Gamma=29$ meV ($m_f\neq1$). The more realistic result of $\Gamma=29$ meV for the total linewidth is in good agreement with the experimentally measured lifetime[35] of 22 ± 3 fs at 25 K.[13,14] Within the vacuum side of the surface the $n=1$ image state couples dominantly to the $n=0$ surface state (this coupling approximately represents 90% of the total Γ_{vac} linewidth); however, the coupling of image states with all bulk crystal states occurring through the bulk penetration plays an important role and cannot, therefore, be neglected if one is to accurately describe the lifetime of image states.

We note that simplified jellium models for the evaluation of the screened interaction lead to unrealistic results for the contribution of the surface state to the linewidth of image states.[36] First, we compare our full RPA calculations (see Table I) with the results we obtain, also with use of our model initial and final wave functions, when our realistic screened interaction is replaced by that obtained within the specular reflection model and the model of Persson and Zaremba. Bulk contributions to the linewidth are approximately well described within the specular reflection model, small differences resulting from an approximate description, within this model, of the so-called *begrenzung* effects. As the approximate treatment of Ritchie and Marusak[25] ignores the quantum-mechanical details of the surface, this model fails to describe both vacuum and interference contributions to the linewidth. These quantum-mechanical details of the surface are approximately taken into account within the jellium model of Ref. 27, thus resulting in a better approximation for the vacuum contribution to the linewidth. Discrepancies between vacuum contributions obtained within this model (PZ) and our more realistic full RPA calculations[36] appear as a result of the jellium model of Ref. 27 being accurate provided $q_\parallel/q_F$ and $\omega/E_F\ll1$ (q_F is the Fermi momentum, i.e., $E_F=q_F^2/2$).

In order to investigate the dependence of Γ_s on the details of both $n=1$ and $n=0$ wave functions, we present in Table I calculations, within SRM and PZ models for the screened interaction, in which our realistic wave functions are replaced by the simplified models (AWF) described in the previous section. As the hydrogeniclike wave function used to describe the $n=1$ image state on the vacuum side of the surface presents an image-state charge-gravity center localized further away from the surface than our more realistic model wave function, both vacuum and interference contributions to the linewidth are largely underestimated within this approximation. Furthermore, we note that the linewidth is highly sensitive to the details of the image-state wave functions. This is a consequence of the critical behavior of the imaginary part of the nonlocal self-energy coupling points near the surface, as we will discuss below.

Now we focus on our full RPA calculation of the total linewidth of the $n=1$ image state on Cu(111) (see Table II), with all effective masses set equal to the free-electron mass. We show in Fig. 2(b) separate contributions to the linewidth, Γ, coming from the decay into the various f bulk crystal states, Γ_f, such that

$$\Gamma=\sum_f \Gamma_f+\Gamma_s. \tag{9}$$

Figure 2(a) exhibits the bulk band structure projected onto the (111) surface of copper. The arrows indicate the available phase space in the decay of the $n=1$ image state at the Γ point ($\mathbf{k}_\parallel=0$) into the unoccupied portion of the $n=0$ surface state and a generic f bulk state, which are represented by their characteristic $\epsilon_0+q_\parallel^2/2$ and $\epsilon_f+q_\parallel^2/2$ parabolic dispersions, respectively. Γ_{vac}, Γ_{sol}, and $-\Gamma_{inter}$ contributions to Γ_f are represented, together with the total contribution Γ_f as a function of ϵ_f.

The lower edge, at the $\bar{\Gamma}$ point, of the energy gap projected onto the Cu(111) surface lies below the Fermi level ($E_g<E_F$) and, consequently, the decay from the ($\mathbf{k}_\parallel=0$) image state occurs through finite-parallel momentum transfer. Hence, as the coupling of the image state with the crystal occurring through the tails of bulk states outside the crystal is expected to be dominated by vertical transitions ($q_\parallel\simeq0$), vacuum contributions to the Γ_f linewidth are very small, especially for those bulk states located at the bottom of the valence band (decay into these states is only allowed for large values of the momentum transfer; also, their vacuum

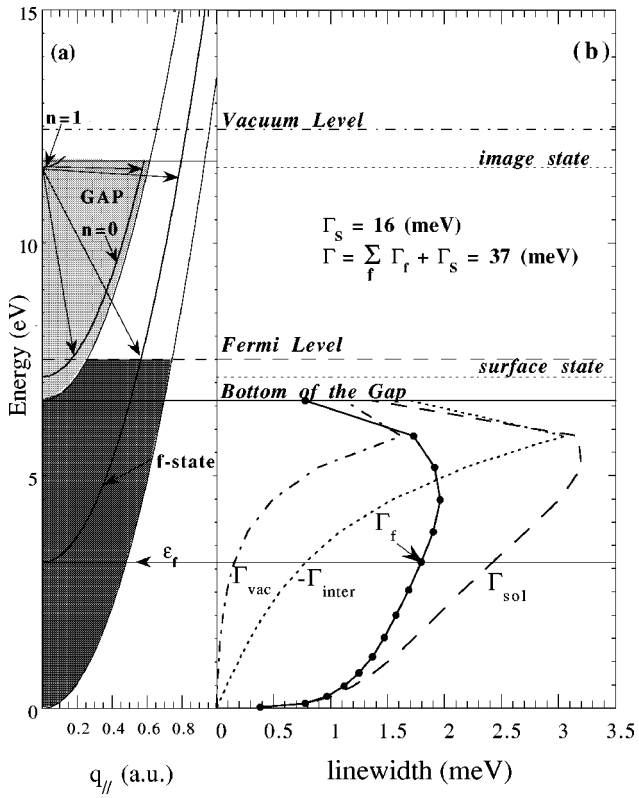

FIG. 2. (a) Electronic-surface band structure at the (111) surface of copper. (b) Vacuum (Γ_{vac}), bulk (Γ_{sol}), and interference ($-\Gamma_{inter}$) contributions to the linewidth (Γ_f) coming from the decay into the various f bulk crystal states. The arrows determine the available phase space in the decay from the $\bar{\Gamma}$ point of the $n=1$ image state into the unoccupied portion of both the $n=0$ surface state and the generic f bulk state. Dispersion curves of these final states are depicted. The energy is measured with respect to the bottom of the valence band. All effective masses have been set equal to the free-electron mass.

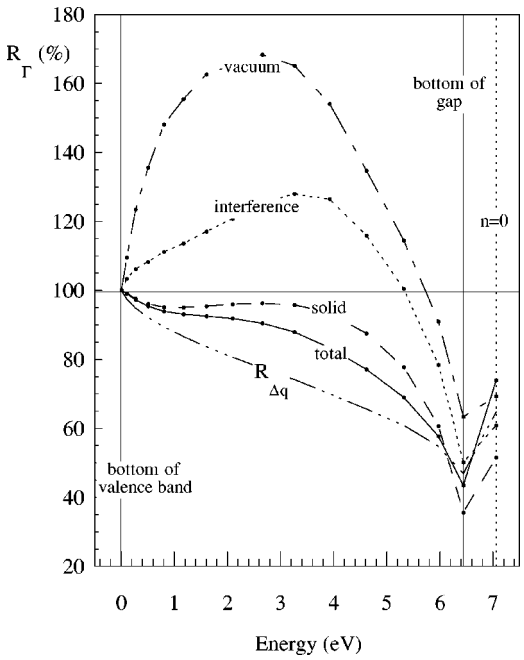

FIG. 3. Ratio R_{Γ_f} of Eq. (10), as a function of the final state energy. The effective mass and the momentum parallel to the surface of the $n=1$ image state have been set equal to the free-electron mass and equal to zero, respectively. As for final (bulk and intrinsic surface) states, we have used the realistic effective masses ($m_f \neq 1$) described in the text. Here, $R_{\Delta q_\parallel} = 100\sqrt{m_f}$.

penetration is small). Actually, the coupling of the $n=1$ image state with all bulk states taking place at the vacuum side results in a linewidth of only 5 meV, which approximately represents 10% of the total Γ_{vac} linewidth.[37]

A realistic description of motion along the surface can be approximated by introduction of the effective mass, as described above. The effective mass of all final states with energies $E_f, E_f \leqslant E_f \leqslant E_1$, is found to be smaller than the free-electron mass, thus both Γ_s and Γ being about 20% smaller than in the case of free-electron behavior along the surface (see Tables I and II). This is the result of two competing effects: First, there is the effect of the decrease of the available phase space, which is easily found to scale as $\sqrt{m}$. Second, as the effective mass decreases the decay from the image state occurs, for a given energy transfer, through smaller parallel momentum transfer, which may result in both enlarged and diminished screened interactions, depending on momentum and energy transfers. This is illustrated in Fig. 3, where the impact of the introduction of the effective mass on the evaluation of the various contributions (vacuum, bulk, and interference) to both Γ_f and Γ_s [see Eq. (9)] is exhibited through the percentage ratio

$$R_{\Gamma_f} = 100 \frac{\Gamma_f(m_f \neq 1)}{\Gamma_f(m_f = 1)}, \tag{10}$$

as a function of the final-state energy ϵ_f. If the screened interaction were independent of the parallel momentum transfer, all ratios would scale as $\sqrt{m}$, which is represented in Fig. 3 as $R_{\Delta q_\parallel} = 100\sqrt{m_f}$. Instead, as the parallel momentum transfer decreases the screened interaction is predominantly larger, which results in the ratio R_{Γ_f} to be larger than $R_{\Delta q_\parallel}$, especially in the case of vacuum contributions to the linewidth, which are expected to be dominated by vertical transitions. When the decay from the image state may occur through very small parallel momentum transfer $q_\parallel$ [this is the case of final states that are just below the bottom of the gap and also the case of the $n=0$ surface state], a decrease in $q_\parallel$ may result in a diminished screened interaction (see Fig. 4), thus R_{Γ_f} being slightly smaller than $R_{\Delta q_\parallel}$ for these states.

Now, we analyze the behavior of the imaginary part of the image-electron self-energy, which results in vacuum and interference contributions to the linewidth to be comparable in magnitude and opposite in sign (see Table I). Figure 5 shows full RPA (solid line) and SRM (dashed-dotted line) calculations of $-\mathrm{Im}\,\Sigma_s(z,z',\mathbf{k}_\parallel=0,E_1)$ [see Eq. (3)] for Cu(111) with all effective masses set equal to the free-electron mass, together with the $n=1$ image-state wave function, as a function of the z'-coordinate and for $z=7.4$ a.u.. We note that the probability for electron-hole pair creation (the dominant channel for the decay of these states is provided by this process) is underestimated within the SRM.

The coupling between electronic states is well known to be maximum, within the bulk, at the position of the electron. Nevertheless, as the electron moves into the vacuum the maximum of the imaginary part of the electron self-energy

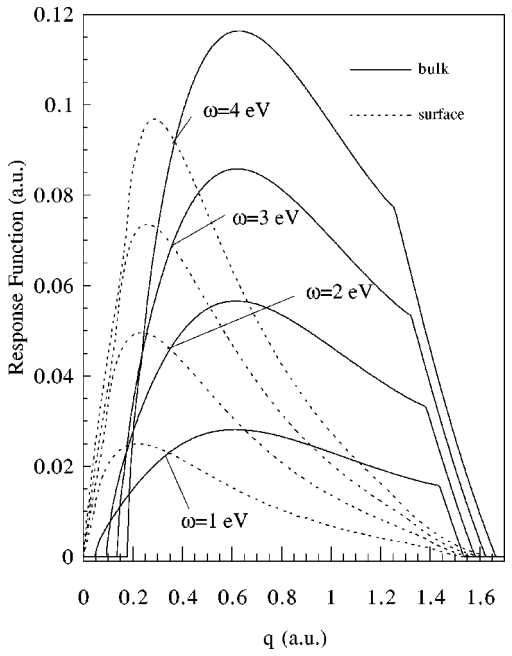

FIG. 4. Imaginary part of bulk (solid lines) and surface (dotted lines) response functions, $\mathrm{Im}[-1/\epsilon(q,\omega)]$ and $\mathrm{Im}[-g_s(q_\parallel,\omega)]$, which describe the screened interaction far from the surface into the bulk and into the vacuum, respectively. Bulk response functions have been evaluated in the RPA, whereas surface response functions have been evaluated within the specular reflection model of the surface (SRM) (Ref. 26) with the RPA for the bulk dielectric function (Ref. 22).

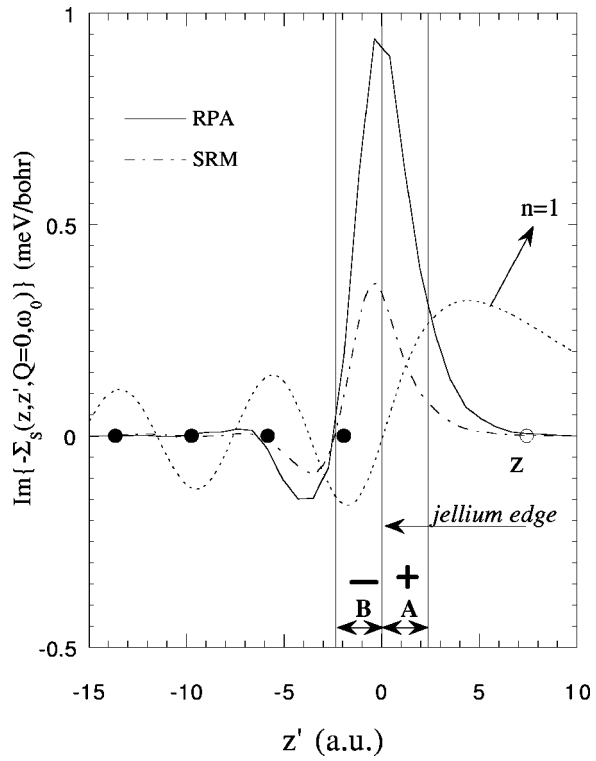

FIG. 5. Full RPA (solid line) and SRM (dashed-dotted line) calculations of $-\mathrm{Im}\,\Sigma_s(z,z',\mathbf{k}_\parallel=0,E_1)$, as obtained from Eq. (3) and as a function of the z' coordinate. The dotted line represents the $n=1$ image-state wave function (MWF). The value of z ($z=7.4$ a.u.) is indicated by an open circle. The sign appearing in regions A and B accounts for the sign of the product between the imaginary part of the self-energy and the image-state wave function. Full circles represent the atomic positions in the (111) direction. The geometrical electronic edge ($z=0$) has been chosen to be located half an interlayer spacing beyond the last atomic layer. All effective masses have been set equal to the free-electron mass.

stays (see Fig. 5) near the surface ($z=0$), as demonstrated, within a jellium model of the surface, by Deisz *et al.*[38] Hence, for any given value of $z>0$, main vacuum and interference contributions to the linewidth are determined [see Eq. (1)] by the specific shape of the image state wave function in regions *A* and *B* of Fig. 5. As the image-state on Cu(111) is located right at the top of the energy gap and the corresponding wave function has, therefore, a node at the surface ($z\simeq 0$), an inspection of Fig. 5 leads us to the conclusion that vacuum and interference contributions to the linewidth are comparable in magnitude and opposite in sign. On Cu(100) the image state is located close to the center of the gap, and the corresponding wave function has a node at $z\simeq 1.3$ a.u. On this surface, total vacuum and interference contributions to the linewidth are still opposite in sign, though interference contributions coming from the decay into states at the bottom of the valence band are now positive due to their minor vacuum penetration. If the image state were located at the bottom of the gap, matching at the surface would occur at maximum amplitude and the total interference contribution might be positive, as the sign of the image-state wave function would be the same on both sides just around the surface ($z=0$).

Finally, we investigate the dependence of interband[23] linewidths on the momentum of the image electron parallel to the surface $\mathbf{k}_\parallel$. First, we use the MWF image-state wave function evaluated at the $\bar{\Gamma}$ point and introduce, within this model, the dependence on $\mathbf{k}_\parallel$ of the quasiparticle self-energy, as indicated in Eq. (2). We find that for image-state total energies lying below the top of the gap ($k_\parallel\simeq 0.11$ a.u.), the linewidth of the first image state of Cu(111) increases less than 4%. Second, we also account for the change of the *z*-dependent initial wave function along the dispersion curve of the image state, by solving the Schrödinger equation for a one-dimensional model potential that we build following Ref. 21 with various values of $k_\parallel$: 0.06, 0.09, and 0.10 a.u.. The penetration into the bulk of the $n=1$ image state with these values of $k_\parallel$ is found to vary from 22.1% at $k_\parallel=0$ to 22.6%, 24.1%, and 26.2% at $k_\parallel=0.06$, 0.09, and 0.10 a.u., respectively. Our results, as obtained with all effective masses set equal to the free-electron mass, are presented in Table III. Though the penetration of the image-state wave function increases with $k_\parallel$, the amplitude of this wave function on the bulk side and near the jellium edge decreases, thus the absolute value of both bulk and interference contributions to the linewidth decreasing with $k_\parallel$. Nevertheless, the total overlap between image-state and final wave functions becomes more efficient as $k_\parallel$ increases, which results in larger values of the total linewidth. Also, it is interesting to notice that especially sensitive to the variation of the momentum of the image state parallel to the surface is the contribution to the linewidth from damping into the $n=0$ surface state.

TABLE III. Calculated total linewidth (in meV) of the first image state on Cu(111), computed within our full RPA scheme with all wave functions computed from the one-dimensional model potential of Ref. 21, as a function of the momentum of the image electron parallel to the surface, $k_\parallel$ (see text). All effective masses have been set equal to the free-electron mass. Contributions to the linewidth from decay into the $n=0$ crystal-induced surface state Γ_s are displayed in parentheses.

$k_\parallel$	$\Gamma_{\rm vac}$	$\Gamma_{\rm sol}$	$\Gamma_{\rm inter}$	Γ
0.0000	47 (42)	44 (16)	−54 (−42)	37 (16)
0.0570	48 (44)	40 (13)	−49 (−38)	39 (19)
0.0912	50 (45)	32 (8)	−38 (−29)	44 (24)
0.1026	50 (44)	28 (6)	−31 (−23)	47 (27)

IV. SUMMARY

We have reported calculations of the inelastic broadening of the first image state at the (111) surface of copper, and we have investigated, in particular, the role that the intrinsic crystal-induced surface state plays in the decay of this image state. We have presented self-consistent RPA calculations, by going beyond a free-electron description of the metal surface. We have also considered simplified models for both the electron wave functions and the screened-Coulomb interaction, showing that a detailed description of these quantities is of crucial importance in the understanding of the origin of linewidths of image states. We have accounted for potential variation parallel to the surface through the introduction of the effective mass.

We have analyzed the origin and magnitude of the various contributions to the linewidth. Though the dominant contribution to the decay of the first image state into the crystal-induced surface state comes from the coupling between image and surface states within the vacuum part of the surface, it appears to be approximately canceled out by the contribution from the interference between bulk and vacuum coordinates. For the vacuum contribution to the decaying rate into the intrinsic surface state, we have found that it approximately represents 90% of the total vacuum contribution. We also conclude that the coupling of image states with all bulk crystal states occurring through the bulk penetration plays an important role in the determination of lifetimes, and that this penetration cannot be neglected if one is to accurately describe the lifetime of image states.

We have found, within our full RPA scheme, that in the case of $\mathbf{k}_\parallel=0$ the decaying rate of the first image state on Cu(111) into the intrinsic surface state results, with all effective masses set equal to the free-electron mass, in a linewidth of 16 meV, while use of more realistic effective masses leads to a linewidth of 12 meV. With the use of either the free-electron mass or more realistic effective masses for both bulk and crystal-induced surface states, Γ_s approximately represents 40% of the total linewidth, $\Gamma=37$ meV ($m_f=1$) or $\Gamma=29$ meV ($m_f\neq1$). The more realistic result of $\Gamma=29$ meV for the total linewidth is in good agreement with recent experimental results reported in Ref. 13.

We have investigated the dependence of interband linewidths on the momentum of the image electron parallel to the surface, showing that for image-state total energies lying below the top of the gap the linewidth of the first image state increases with $k_\parallel$ up to 20%. We conclude that this increase appears mainly as a consequence of the change of the z-dependent initial wave function with $k_\parallel$, and our results indicate that the contribution to the linewidth from damping into the $n=0$ surface state is responsible for the dependence of the total linewidth with the momentum parallel to the surface.

ACKNOWLEDGMENTS

The authors gratefully acknowledge A. Rubio, E. Zarate, and M.A. Cazalilla for fruitful discussions in connection with this research. This project has been supported by Eusko Jaurlaritza (Basque Country), the Ministerio de Educación y Cultura (Spain), and Iberdrola S.A.

[1] P.M. Echenique and J.B. Pendry, J. Phys. C **11**, 2065 (1978); Prog. Surf. Sci. **32**, 111 (1990).
[2] Th. Fauster and W. Steinmann, in *Photonic Probes of Surfaces*, edited by P. Halevi (Elsevier, Amsterdam, 1995), pp. 347–411.
[3] R.M. Osgood, Jr. and X. Wang, Solid State Phys. **51**, 1 (1997), and references therein.
[4] E.V. Chulkov, V.M. Silkin, and P.M. Echenique (unpublished).
[5] F. Passek and M. Donath, Phys. Rev. Lett. **69**, 1101 (1992).
[6] F. Passek, M. Donath, K. Ertl, and V. Dose, Phys. Rev. Lett. **75**, 2746 (1995).
[7] R.W. Schoenlein, J.G. Fujimoto, G.L. Eesley, and T.W. Capehart, Phys. Rev. Lett. **61**, 2596 (1988).
[8] S. Schuppler, N. Fischer, Th. Fauster, and W. Steinmann, Phys. Rev. B **46**, 13 539 (1992).
[9] X.Y. Wang, X.J. Shen, R.M. Osgood, Jr., R. Haight, and F.J. Himpsel, Phys. Rev. B **53**, 15 738 (1996).
[10] T. Hertel, E. Knoesel, M. Wolf, and G. Ertl, Phys. Rev. Lett. **76**, 535 (1996).
[11] M. Wolf, E. Knoesel, and T. Hertel, Phys. Rev. B **54**, 5295 (1996).
[12] J.D. McNeill, R.L. Lingle, Jr., N.-H. Ge, C.M. Wong, R.E. Jordan, and C.B. Harris, Phys. Rev. Lett. **79**, 4645 (1997).
[13] E. Knoesel, A. Hotzel, and M. Wolf, J. Electron Spectrosc. Relat. Phenom. **88-91**, 577 (1998).
[14] I.L. Shumay, U. Höfer, Ch. Reuß, U. Thomann, W. Wallauer, and Th. Fauster, Phys. Rev. B **58**, 13 974 (1998).
[15] U. Höfer, I.L. Shumay, Ch. Reuß, U. Thomann, W. Wallauer, and Th. Fauster, Science **227**, 1480 (1997).
[16] P.M. Echenique, F. Flores, and F. Sols, Phys. Rev. Lett. **55**, 2348 (1985).
[17] P. de Andrés, P.M. Echenique, and F. Flores, Phys. Rev. B **35**, 4529 (1987).
[18] S. Gao and B.I. Lundqvist, Prog. Theor. Phys. Suppl. **106**, 405 (1991); S. Gao and B.I. Lundqvist, Solid State Commun. **84**, 147 (1992).
[19] E.V. Chulkov, I. Sarría, V.M. Silkin, J.M. Pitarke, and P.M. Ech-

enique, Phys. Rev. Lett. **80**, 4947 (1998).
[20] L. Hedin and S.O. Lundqvist, in *Solid State Physics*, edited by F. Seitz, H. Ehrenreich, and D. Turnbull (Academic, New York, 1969), Vol. 23, p. 2.
[21] E.V. Chulkov, V.M. Silkin, and P.M. Echenique, Surf. Sci. Lett. **391**, 1217 (1997).
[22] See, e.g., D. Pines, *Elementary Excitations in Solids* (Addison-Wesley, New York, 1963), Chap. 3.
[23] In these processes the image electron decays into a state having a different z-dependent (the plane of the surface is assumed to be perpendicular to the z axis) wave function.
[24] The effective mass of the image state is taken to be equal to the free-electron mass, i.e., $m_1=1$ (see, e.g., Ref. 2).
[25] R.H. Ritchie and A.L. Marusak, Surf. Sci. **4**, 234 (1966).
[26] P.M. Echenique, F.J. García de Abajo, V.H. Ponce, and M.E. Uranga, Nucl. Instrum. Methods Phys. Res. B **96**, 583 (1995).
[27] B.N.J. Persson and E. Zaremba, Phys. Rev. B **31**, 1863 (1985).
[28] A. Goldmann, V. Dose, and G. Borstel, Phys. Rev. B **32**, 1971 (1985).
[29] S.D. Kevan, Phys. Rev. Lett. **50**, 526 (1983).
[30] S.L. Hulbert, P.D. Johnson, N.G. Stoffel, W.A. Royer, and N.V. Smith, Phys. Rev. B **31**, 6815 (1985).
[31] The electron-density parameter has been taken to be $r_s=2.58$, so as to reproduce the Fermi energy of 7.53 eV obtained within our model calculation of the ground state.
[32] The parameters entering the surface response function of Persson and Zaremba (Ref. 27) have been taken to be $m_{opt}=1.68$, $h=1.84$, and $\xi=0.49$.
[33] *Ab initio* calculations of the bulk band structure have been projected onto the (111) surface of copper, and the dispersion $E(k_\parallel)$ along the $\bar{\Sigma}:\bar{\Gamma}\rightarrow\bar{\mathrm{M}}$ direction has been fitted to $E_\parallel=k_\parallel^2/(2m)$ with $m=0.22$ and $m=3.8$ at the bottom and the top of the gap, respectively. Though the effective mass at the bottom of the gap has been reported (Ref. 34) for Cu(111) to be $m=0.31$, our calculation of the lifetime is nearly insensitive to the precise choice of either $m=0.22$ or $m=0.31$ of Ref. 34.
[34] S.D. Kevan and R.H. Gaylord, Phys. Rev. B **36**, 5809 (1987).
[35] The lifetime τ is related to the linewidth Γ of Eqs. (1) and (4) by $\Gamma\tau=\hbar=660$ meV fs.
[36] We find that the impact of the band structure in the evaluation of the screened interaction is not large, and differences between our full RPA calculations, on the one hand, and the SRM and PZ results, on the other hand, appear as a consequence of simplifications introduced, within a jellium model of the surface, in both SRM and PZ approaches.
[37] Notice that both Γ_{vac} and Γ_{inter} contributions to the linewidth present a maximum for energies just below the bottom of the energy gap. This is due to the fact that the vacuum penetration of the bulk states increases as one goes up in energy and then decreases just below the gap due to the stronger bulk character of these states reproducing the bottom of the gap. This maximum appears here as a cusp because of the relatively thin slab used in the present calculation. This sharp feature will be significantly smoother for thicker films.
[38] J.J. Deisz, A.G. Eguiluz, and W. Hanke, Phys. Rev. Lett. **71**, 2793 (1993).